ANALYSIS OF ROTORCRAFT PILOT COUPLINGS FROM THE FLIGHT CONTROL SYSTEM MODES PERSPECTIVE

Ying Yu, Y.Yu-2@tudelft.nl, Technical University Delft, The Netherlands, Politecnico di Milano, Italy

Marilena D. Pavel, M.D.Pavel@tudelft.nl, Technical University Delft, The Netherlands

Erik-Jan van Kampen, E.vanKampen@tudelft.nl, Technical University Delft, The Netherlands

Pierangelo Masarati, Pierangelo.Masarati@polimi.it, Politecnico di Milano, Italy

Abstract

This paper investigates Rotorcraft Pilot Coupling (RPC) with different Flight Control System (FCS) modes. A generic 16DOF nonlinear helicopter model configured with Rate Command Attitude Hold (RCAH), Attitude Command Attitude Hold (ACAH) and Translational Rate Command (TRC) mode has been developed to run simulations on triggering PIO. In addition, ROVER has been extended to multi-axis ROVER to detect PIO. The control mode sensitivity and tolerability to pilot time delay, actuator saturation, actuator rate limit, control authority of the Stability and Control Augmentation System (SCAS) and sensor dynamics are studied. Results show that: 1) the tolerance to the pilot time delay is highest for the TRC mode, followed by ACAH and RCAH; 2) inner vehicle trigger factors (actuator saturation, actuator rate limit, control authority and sensor dynamics) play a more important role than external trigger factors (pilot time delay) in triggering PIO; 3) inner vehicle trigger factors make the RCAH, ACAH and TRC mode more sensitive to pilot time delay; 4) the tolerability of different control modes to abnormal actuator saturation is the same; 5) for actuator rate limit and control authority, the TRC mode has the highest tolerance, followed by ACAH and RCAH; 6) TRC mode and RCAH mode have the same tolerability to abnormal sensor dynamics while the tolerability of ACAH is lower. These findings offer guidance for designing pilot-in-the-loop simulator experiments that will further investigate RPCs related to different control modes.

Nomenclature

p	Roll rate
q	Pitch rate
r	Yaw rate
ϕ	Roll angle
θ	Pitch angle
ψ , ψ_{com}	Yaw angle, command
V_{x} , V_{xcom}	Ground forward speed, command
V_{y} , V_{ycom}	Ground lateral speed
V_{z} , V_{zcom}	Ground vertical speed
h	Altitude
$\theta_{1\text{s}}$	Longitudinal control input
$\theta_{1\text{c}}$	Lateral control input
$\theta_{0\text{mr}}$	Collective control input
$\theta_{0\text{tr}}$	Tail rotor control input
τ_{p}	Pilot time delay
τ_{bp}	Phase delay
ω_{BWgain}	Gain bandwidth
ω_{BWphase}	Phase bandwidth
ω_{BW}	Bandwidth
ω_{n}	Natural frequency of the
ξ	Damping for the neuromuscular
s	Laplace operator

Presented at 45th European Rotorcraft Forum, Warsaw, Poland, 17–19 September, 2019.

ω_{sn}	Natural frequency of sensor
ξ_{sn}	Damping for the sensor dynamics

Acronyms

ACAH	Attitude Command Attitude Hold
ADS	Aeronautical Design Standard
AS	Actuator Saturation
CA	Control Authority
DOF	Degree of Freedom
RPC	Rotorcraft Pilot Coupling
FBW	Fly-by-wire
FCS	Flight Control System
HQ	Handling Qualities
PID	Proportional Integrative Derivative
PIO/PAO	Pilot Induced/Assisted Oscillation
PIW	Pilot-Inceptor Workload
PTD	Pilot Time Delay
PVS	Pilot Vehicle System
RCAH	Rate Command Attitude Hold
ROVER	Real-Time Oscillation VERifier
RL	Rate Limit
SCAS	Stability and Control Augmentation
SD	Sensor Dynamics
TRC	Translational Tate Command

1. INTRODUCTION

According to the accident investigation reports of the International Helicopter Safety Team (IHST), pilot loss of control is the most prominent factor that endangers helicopter safety[1,2]. There are many reasons accounting for pilot loss of control, such as inappropriate pilot control strategies and helicopter system failures[3]. Within the pilot loss of control category, rotorcraft-pilot couplings (RPCs) is an area of particular interest. Rotorcraft pilot couplings, known in the past under the name pilot induced/assisted oscillations (PIO/PAO), are undesired vehicle oscillations arising from the pilot coupling to the vehicle dynamics when triggered by a particular factor[4]. This does not mean that the pilot is specifically at fault, since shortcomings of the helicopter itself can result in unintended oscillations. Those shortcomings can be regarded as inner vehicle trigger events of PIO. Within RPC instabilities, the so-called Cat. III PIO depends on nonlinear transitions in either the controlled element (such as flight control mode changes, internal FCS changes, aerodynamic or propulsion configuration changes) or in the pilot's dynamics, is probably the most complicated RPC to be solved[5, 7, 8]. The research of pilot modelling is beyond the scope of this paper. This paper will mainly focus on trigger events inside the controlled element.

Fly-By-Wire (FBW) flight control systems are widely used in modern vehicles[11]. It is a double-edged sword. One the one hand, its multi-redundant flight control modes can help reduce the pilot's workload, and on the other hand, unexpected flight control mode transitions may lead to the nonlinear Cat. III PIO. The reason why mode transition causes PIO may be the sensitivity or the tolerability of different control modes to the inner vehicle triggers. The study of control mode sensitivity or tolerability to vehicle trigger factors is therefore of great importance.

In order to get some understanding of the problem, a 16-DOF nonlinear model (including body dynamics, second-order flapping dynamics, Pitt-Peters inflow dynamics for the main rotor and first order inflow dynamics for the tail rotor)[9] is built in the MATLAB/Simulink software environment. Three different flight control modes or response types are designed: rate command attitude hold (RCAH), attitude command attitude hold (ACAH) and translational rate command (TRC). RCAH has the characteristics that a pilot's constant deflection creates a constant angular rate. In ACAH mode, a constant deflection of pilot input creates a constant attitude angle. With TRC, a constant deflection of the pilot's input creates a constant vehicle ground velocity[12]. These "Response Types" are defined in detail in ADS-33E-PRF[10]. All flight control modes designed in this research are based on PID control. This paper will consider different control mode sensitivity or tolerability to some of the potential RPC triggers (pilot time delay, actuator saturation, actuator rate limit, control authority, and sensor dynamics) which was studied in the literature[6].

Another important element is to detect PIO. The premise of detecting PIO is to reach a consensus on the definition of PIO. Mitchell summarized ten common definitions of PIO in the literature[13]. Then a more detailed definition of PIO is proposed as "*PIO is a sustained or uncontrollable unintentional oscillation in which the airplane attitude, angular rate, normal acceleration, or other quantity derived from these states, is approximately 180 degrees out of phase with the pilot's control inputs.*" This definition clearly points out the most important characteristic of PIO: the vehicle response is out of phase with pilot input.

As for PIO detection methods, there are numerous methods for detecting Cat. I PIO (such as Neal-Smith, Smith-Geddes, Gibson, Bandwidth/Pitch Rate Overshoot, Time Domain

Presented at 45th European Rotorcraft Forum, Warsaw, Poland, 17-20 September 2019

Neal-Smith)[14] and Cat. II PIO (such as Bandwidth/Pitch Rate Overshoot, Open-Loop Onset Point, Pilot/Vehicle Dynamics Non-Linear, Time Domain Neal-Smith)[14], but hardly any method is specialized for detecting Cat. III PIO. The application, strengths, and weaknesses of the aforementioned criteria can be found in reference[14]. The best criteria among the ones mentioned in reference[14] is the Bandwidth/Pitch Rate Overshoot criteria. However, it requires an accurate frequency response, whereas nonlinearities reduce the quality of the frequency response. Furthermore, nonlinearities such as rate limits are amplitude and frequency-dependent, which means a family of solutions rather than a single point must be considered. Thus it increases the complexity of its application. In reference[15] it is pointed out that operation not around trim values does not indicate reliable HQ levels according to ADS-33. Therefore, for the highly nonlinear helicopter considered in this paper, the Bandwidth criteria may not apply.

In addition, a real-time (or quasi-real-time) detection method denoted as Real-Time Oscillation VERifer (ROVER) was developed almost two decades ago for the U.S. Air Force[17]. It detects PIO based on four parameters: oscillation frequency, vehicle response magnitude, pilot input magnitude, and phase lag between pilot input and vehicle response. Although one drawback of ROVER is that it can be prone to false alerts due to the fact that its thresholds for PIO detection must be predefined by the user, it can still be regarded as an effective way to detect PIO since it conforms to the definition of PIO well.

Subsequently, Michael proposed a new real-time (or quasi-real-time) detection method “Phase Aggression Criterion (PAC)”[8] by extending the Pilot-Inceptor Workload (PIW) criterion[19] with the phase difference between pilot input and vehicle rate output. This method is similar to ROVER since the way in which PAC calculates the phase difference is inherited from ROVER. The difference between them is that PAC uses a new index, named “pilot aggression” to indicate the pilot control activity, whereas ROVER only uses the pilot input amplitude to indicate the aggressiveness of the pilot. The advantage of PAC over ROVER is that it removed the need for a subjective selection of thresholds. However, PAC introduced new subjectivities since the boundaries it obtained were based on test pilots’ comments and subjective ratings. Thus, it is difficult to evaluate whose subjectivity is more straightforward to deal with. Furthermore, the PAC results have been restricted to Rate Command systems currently and its application to other control modes needs further investigation[8], especially the update of the so-called boundaries. The PAC boundaries may be only effective to the specified vehicle types, configurations and flying tasks etc., since its boundaries can be affected by numerous factors such as control gearing, trigger events (for example, the boundary was based on the Rate Limit, as the limit changes, the position of the boundaries should also change[8]), the investigated axis and so on. The application to Cat. III PIO is questionable and needs further study as well.

Although PIO is classified as Cat. I (linear), Cat. II (quasi-linear) and Cat. III (nonlinear), i.e. according to the reasons that caused PIO, the characteristics of PIO should be the same regardless of categories. Therefore, ROVER is utilized in this research as the detection method since it conforms to the definition of PIO well and it is easy to implement. In addition, the classical single input single output ROVER is extended to be a multi-axis ROVER by doing the union of all single-axis ROVER detection results to obtain final detection results, which will be explained in the following part.

Concluding, the aim of this paper is to give a basic understanding of rotorcraft pilot coupling problems from the FCS control modes perspective. The focus is on control mode sensitivity or tolerability to vehicle trigger factors and pilot time delay and their influence. Finally, the paper will elaborate on whether advanced FCS modes can help to avoid/ alleviate the triggered RPC.

This paper is structured as follows. It begins with a description of the pilot vehicle system and flying tasks utilized in this research in Section 2, followed by the detection method ROVER in Section 3. Results from the MATLAB/Simulink and analysis are then presented in Section 4. Finally, it closed with a description of the ongoing work and some concluding remarks in Section 5.

2. PILOT VEHICLE SYSTEM

The structure of the pilot vehicle system built in MATLAB/Simulink is shown in
Figure **1**. The pilot is assumed to only control the longitudinal and lateral axis, while the other two axes are controlled by the automatic flight control system (AFCS) which is shown by the altitude hold and the heading hold block. A partial authority SCAS is used to help control and stabilize the helicopter, it is the control mode block in the figure. The pilot and SCAS inputs are added to generate the input to the actuator. The 16-DOF nonlinear helicopter model is inherited from Ref[9].

Presented at 45th European Rotorcraft Forum, Warsaw, Poland, 17-20 September 2019

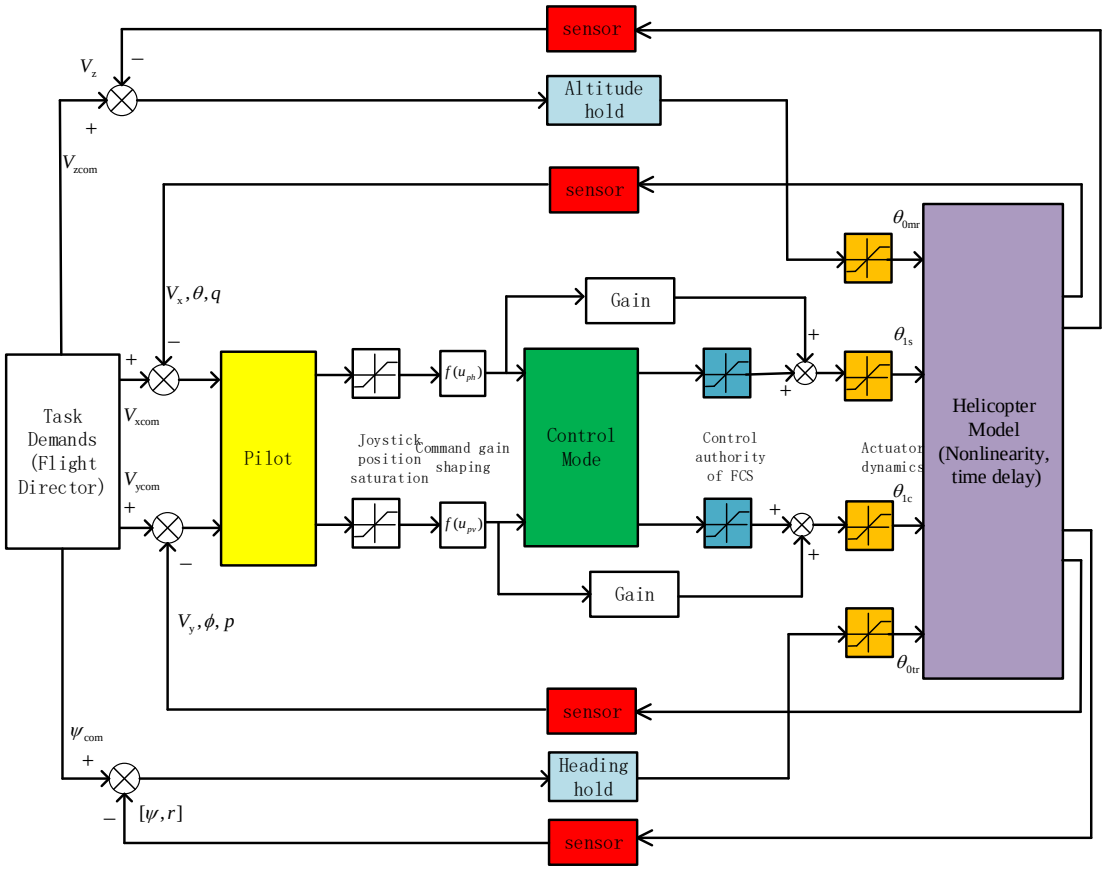

Figure 1 Structure of the pilot vehicle system

2.1 Flight Control System (FCS) control modes and pilot model

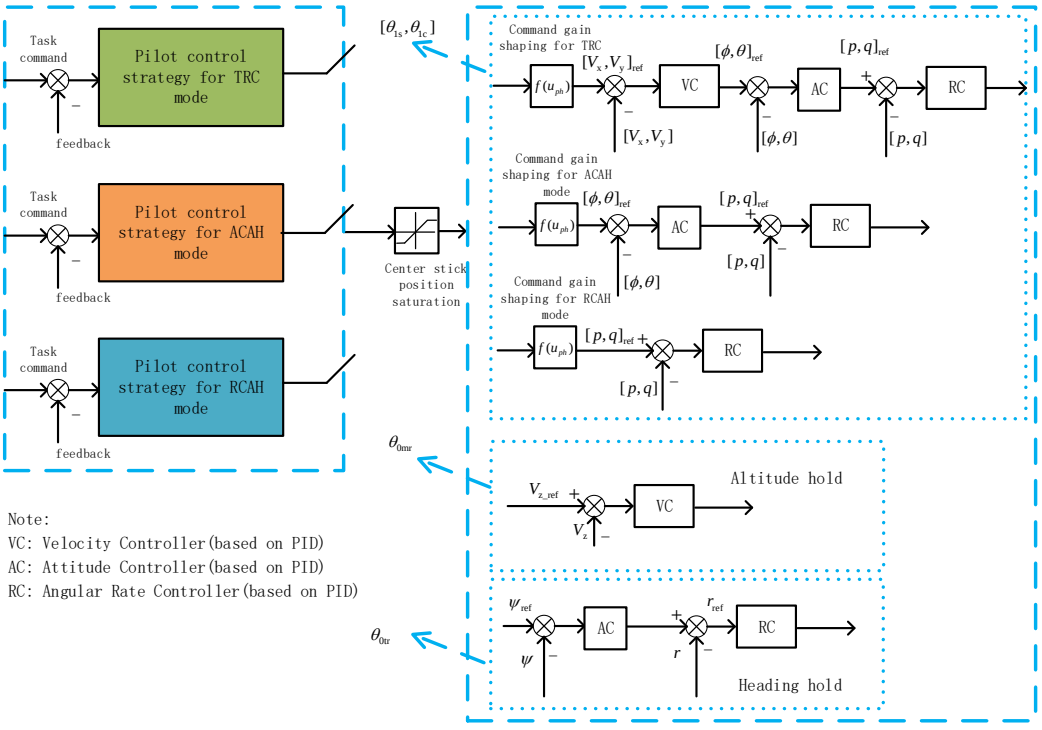

Figure 2. Structure of FCS modes for the 16 DOF helicopter model

Presented at 45th European Rotorcraft Forum, Warsaw, Poland, 17-20 September 2019

The structure of the FCS modes is depicted in Figure 2, which corresponds to the control mode, altitude hold and heading hold blocks in

Figure **1**. The command gain shaping for different control modes is similar to what appears in the literature[6]. The range of pilot stick position is set to be [-50% 50%]. Due to helicopter coupling, a simple pilot model or McRuer model (functions like a PID controller) or other type pilot model cannot guarantee good performance of the tasks that are implemented in this research. In order to accomplish the flying tasks as required and exclude the error from the pilot that will cause PIO, the pilot model used in this research is set to be a nonlinear pilot control strategy plus pilot time delay and pilot physical limitation block. Thus, the pilot model can be depicted as

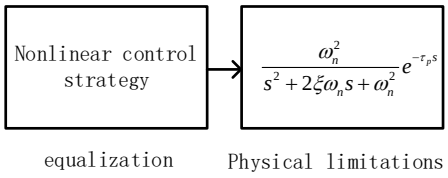

Figure 3. Pilot Model

Where, ω_n is the natural frequency of the neuromuscular system, ξ represents the damping for the neuromuscular system, τ_p is the pilot response delay, and s denotes the Laplace operator and the typical value $\omega_n = 20\text{rad/s}, \xi = 0.7$ is used here[16]. The nonlinear control strategy is generated by a nonlinear block between the flying tasks and pilot physical limitation. Its function is similar to a flight director that gives the pilot the information needed.

2.2 Flying tasks

The flying task is set to be a 3211 signal reference with a period T=20s and amplitude equal to 10m/s in the longitudinal axis. For the lateral axis, the task is set to be $V_{ycom} = 0$. The other two axes are in altitude hold and heading hold mode, that is, $V_{zcom} = 0, \psi_{com} = 0$. The forward ground speed command is shown in Figure 4. A first-order low-pass filter is used for the command signal to generate the desired signal. The helicopter starts in a hover state.

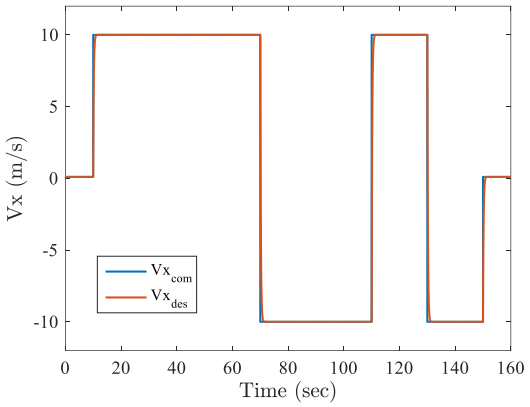

Figure 4. Flying tasks

2.3 Miscellaneous settings

Actuator position saturation, rate limit and sensor dynamics are unavoidable in actual vehicles.

The actuator dynamics are reduced to be a first-order term: $\frac{62.83}{s+62.83}$ and their physical limits are listed in Table 1[9]. To keep it simple in this article, they are normalized as 100% of the physical limits. Other values narrower than the range of the physical limits are denoted as abnormal. For example, [-2*50% 20*50%] represents that the position saturation of collective control is 50% of the physical limits.

Table 1. Actuator parameters[9]

Actuator	Position saturation (deg)	Rate limit (deg/s)
Collective control θ_{0mr}	[-2 20]	[-16 16]
Longitudinal control θ_{1s}	[-6 11]	[-28.8 28.8]
Lateral control θ_{1c}	[-4.2 5.7]	[-16 16]
Tail rotor control θ_{0tr}	[-8 20]	[-32 32]

The sensor dynamics are represented by a second-order term: $\frac{\omega_{sn}^2}{s^2+2\xi_{sn}\omega_{sn}s+\omega_{sn}^2}$, where ω_{sn} represents the natural frequency of the sensor system, ξ_{sn} denotes the damping of the sensor system. In this research, $\xi_{sn} = 0.7$, $\omega_{sn} = 100\text{rad/s}$ is their maximum value and it is 100% of the physical limits. Other values less than 100rad/s are regarded as abnormal condition.

There is no uniform definition of control authority, and the 100% control authority concept in this paper

Presented at 45th European Rotorcraft Forum, Warsaw, Poland, 17–19 September, 2019.

refers to the whole actuator range. For example, for longitudinal control, when removing the trim value of the actuator, its movement range is [-8.5 8.5], which corresponds to a control authority of [-100% 100%]. A control authority of 50% in this paper is calculated as [-8.5*50% 8.5*50%]. Those rules apply to the other actuators as well.

3. DETECTION METHOD ROVER

3.1 Description of ROVER

The Realtime Oscillation VERifier (ROVER) method was first developed for the U.S Air Force[13,17]. One basic assumption behind ROVER is that PIO will never be prevented in real-time and the so-called "pre-PIO condition" does not exist. Moreover, ROVER assumes that every vehicle response is an oscillation.

According to the more specific definition presented in[13,14], four necessary conditions must be met to declare a PIO: 1). There must be an oscillation. Although oscillatory behaviour cannot be taken alone to declare a PIO it remains to be an indispensable element of PIO. 2) The vehicle must be out of phase with the pilot input. This is the most important characteristics to differentiate PIO from normal oscillatory behaviour as a side effect of the normal piloted operation. 3) The frequency of the oscillation must be within the range where PIO appears (Approximately 1-8rad/s). 4) lastly, the amplitude of pilot control inputs, vehicle responses, or both, must be large enough to be noted by the pilot. Small amplitude oscillations may not be regarded as PIO by the pilot.

The algorithm flowchart of ROVER is shown in Figure 5. From the figure, one can see that the two inputs (pilot control input and the selected vehicle response) must be pre-processed by using a low-pass filter to remove high-frequency noise and data spikes. The specific algorithms about the calculation of ROVER parameters: the peak amplitude of pilot control input and vehicle response, the oscillation frequency and phase lag between the pilot control input and vehicle response can be found in Ref[13,14,15]. The calculated values of amplitude, frequency and phase lag are checked against predefined threshold values and a score is issued depending on the number of thresholds crossed. Simply, the final output of ROVER is the algebraic addition of the four flags presented in Figure 5.

In order to reduce the number of false alerts from ROVER, an extra condition is added when calculating the final flag score of ROVER. Considering that two prerequisites for PIO are : 1) the oscillation frequency is in the range of PIO 2) the phase lag between the pilot control input and the selected vehicle response is out of phase. The algebraic addition logic is modified to be: as long as the oscillation frequency flag or the phase lag flag is zero, even the remaining flag all equals one, the sum of the four flags equals two point five (2.5). In this way, the importance of the oscillation frequency and phase lag is increased and it is also differentiated from the case that both the oscillation frequency and phase lag condition are not satisfied. In addition, to increase the warning function of the final flag score when it equals three, the final flag score will be changed to three point five (3.5) if the flag score of three occurs consecutively. This also applies to the consecutive occurrence of three and three point five.

Table 2. Final flag score meaning

Final flag score	PIO
0	No
1	No
2	No
2.5	No
3	precursor
3.5	precursor
4	Yes

Therefore, the final flag score of ROVER has seven cases: flag equals zero, one, two, two point five, three, three point five and four. The meaning of the aforementioned flag score is listed in Table 2. When the final flag equals four, it indicates the occurrence of PIO. Three and three point five means that the pilot is approaching PIO although there is no PIO currently.

ROVER is simple and effective. It is used as a valuable tool for analysing historical flight research and ground simulation data[13]. The shortcoming of ROVER is that the threshold settings of the four flags need to be predefined by the user and the threshold values need to vary to adapt to different vehicle types and configurations and flying tasks and so on. For example, the threshold value for longitudinal and lateral tasks may be different[15]. In addition, the order of the low-pass filter and the cut-off frequency influences the selection of the threshold value. Threshold values are usually chosen after inspection of simulator trials for numerous cases. Last but not least, with the flag score of ROVER only, the severity of PIO (slight, moderate, severe or divergent) cannot be differentiated.

Presented at 45th European Rotorcraft Forum, Warsaw, Poland, 17-20 September 2019

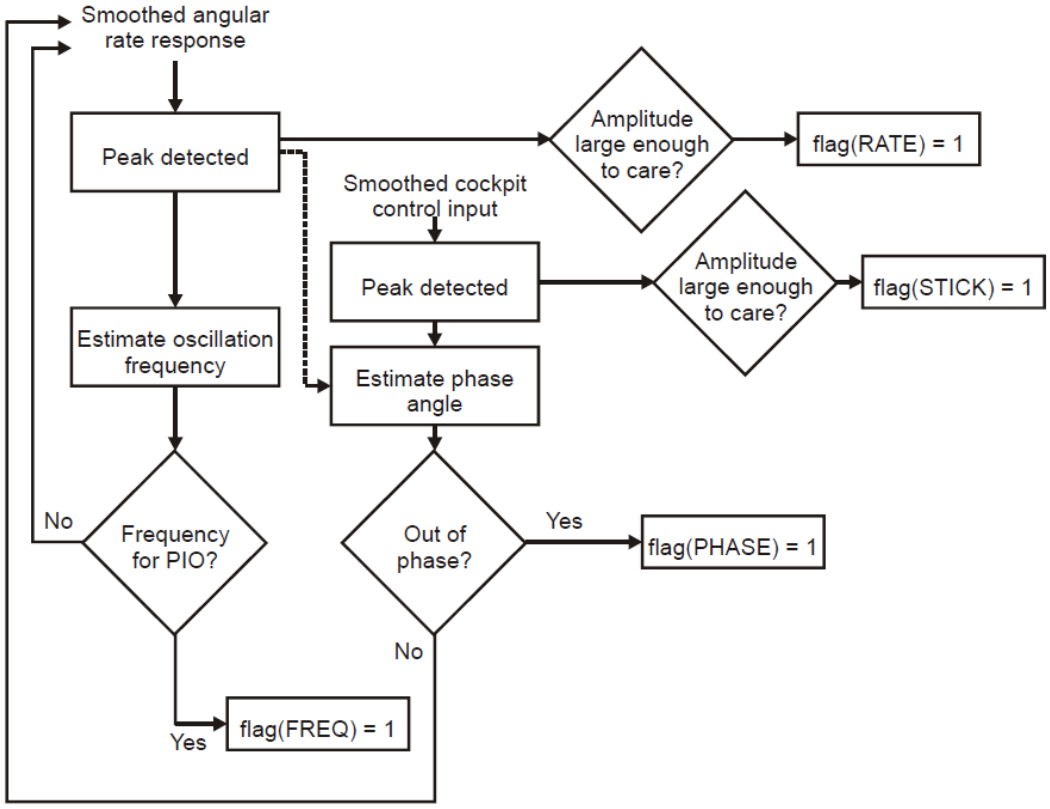

Figure 5. Flowchart for ROVER PIO detection method (originated from Ref[13])

3.2 Multi-axis ROVER

From the definition of PIO, one can know that the vehicle response used for detecting PIO is not assigned specifically, which means any vehicle response can be the input of ROVER. This applies to pilot input as well since the pilot manipulates the vehicle with four channels. Furthermore, there is no evidence to suggest that the vehicle responses having PIO simultaneously which means the vehicle response may suffer from PIO at a different moment. Therefore, for a nonlinear helicopter model with four-channel control input, at least it is necessary to detect PIO in every axis.

As stated in Ref[14,18], the most commonly used states are the attitude angles. However, to monitor angular attitude is challenging since it has non-zero mean and can have relatively small amplitudes at the start of a PIO[14]. The vehicle responses selected to be the input of ROVER are angular rates. Although there are four control channels in the helicopter, the detection of PIO with roll axis, pitch axis, and yaw axis can guarantee the integrity of detection because the vertical velocity can be derived from body velocity and attitude angles. Due to helicopter couplings, the pilot input of any axis can influence vehicle states in all the axes. Hence, all angular rates must be checked with pilot input in each axis one by one. The result of only one angular rate and a single-axis pilot input is named as single-axis ROVER in this paper. Then, the union of all the single-axis ROVER detection results is the final detection result of the whole pilot vehicle system. The final detection result is denoted as the Multi-axis ROVER detection result. In this way, the traditional single input single output ROVER algorithm is extended to be the Multi-axis ROVER. Not only can the Multi-axis ROVER detect the vehicle states having PIO, but it can also pinpoint which pilot control input caused it.

4. RESULTS AND ANALYSIS

4.1 Baseline parameters and performance

In order to get some understanding of the aforementioned pilot vehicle system and different control modes (RCAH, ACAH, TRC), the baseline of each control mode is established, and parameters of corresponding elements are listed in Table 3. In the baseline condition, pilot time delay is set to be zero, and other elements are at their maximum capability (normal physical limit). When they are at the maximum values, it is in normal condition. Other values less than the maximum values are denoted as abnormal condition as stated in Section 2.3.

Presented at 45th European Rotorcraft Forum, Warsaw, Poland, 17–19 September, 2019.

Table 3. Baseline parameters

case	Pilot time delay PTD(ms)	Actuator saturation AS(%)	Rate limit RL(%)	Control authority CA(%)	Sensor dynamics SD ω_{sn} (rad/s)
RCAH-Baseline	0	100	100	100	100
ACAH-Baseline	0	100	100	100	100
TRC-Baseline	0	100	100	100	100

4.1.1 Baseline Handling Qualities

ADS-33 stipulates different methods to evaluate the handling qualities (HQ) of different control modes. As for RCAH and ACAH mode, one effective way to evaluate handling qualities is to use the Bandwidth criteria and its boundaries proposed in ADS-33E-PRF[10]. According to the definition in ADS-33E-PRF, bandwidth and phase delay of different control modes in the baseline condition are calculated and shown in Table 4. From this table, one can see that the bandwidths in the table are beyond the reference range given in ADS-33E-PRF (see Figure 6). This is due to the differences between the model built in MATLAB and the actual vehicle. Some real-life delays in the controllers/sensors/actuators and other unmodelled vehicle dynamics are neglected in this research. Despite the above differences, the bandwidth criteria can still be regarded as a reference. At least, a relative tool for comparison. The handling qualities of the RCAH and ACAH baselines all belong to Level 1.

Table 4. Bandwidth criteria results of baseline

case	ω_{BWgain} (rad/s)	$\omega_{BWphase}$ (rad/s)	ω_{BW} (rad/s)	Phase delay τ_{bp} (s)
RCAH-baseline (longitudinal)	7.57	8.56	7.57	0.04
RCAH-baseline (lateral)	4.40	23.69	4.40	0.04
ACAH-baseline (longitudinal)	7.80	8.73	8.73	0.04
ACAH-baseline (lateral)	5.54	21.63	21.63	0.04

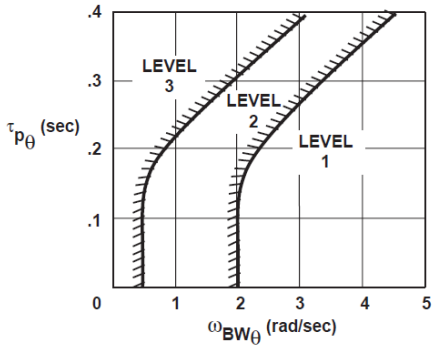

a) Target Acquisition and Tracking (pitch)

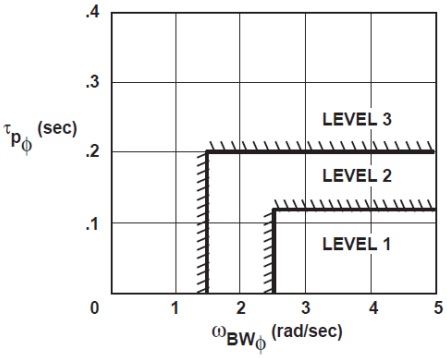

b) Target Acquisition and Tracking (roll)

Figure 6. Requirements for small-amplitude pitch (roll) attitude changes –hover and low speed(originated from ADS-33[10])

As for TRC mode, ADS-33E-PRF states that the translational rate response to step inputs shall have a qualitative first-order appearance and shall have an equivalent rise time between 2.5 seconds and 5 seconds[10]. Thus, in order to check the handling qualities of the TRC mode, simulation of time-domain performance is needed.

4.1.2 Time-domain performance

There is no uniform standard for time-domain performance. Time-domain performance is usually evaluated by its stability and quickness. In this research, rise time and settling time are utilized to evaluate its quickness, steady-state error for its stability, and overshoot for its dynamic process. The baseline time-domain performance of different control modes is shown in Table 5. From this table,

Presented at 45th European Rotorcraft Forum, Warsaw, Poland, 17-20 September 2019

one can see that the differences among control modes is very small. It is worth noting that the rise time is the equivalent rise time in ADS-33, which is defined in Figure 7. The rise time of the TRC baseline is 2.76 seconds, which complies to the Level 1 handling qualities. Therefore, RCAH, ACAH, and TRC baseline are all Level 1.

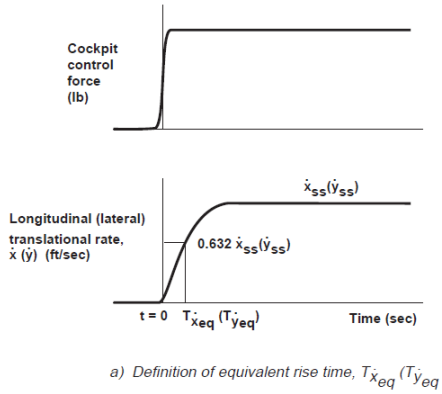

a) Definition of equivalent rise time, $T_{\dot{x}_{eq}}$ ($T_{\dot{y}_{eq}}$)

Figure 7.Definition of equivalent rise time (from ADS-33[10])

Table 5. Time-domain performance of baseline

Case	Rise time(s)	Settling time(s)	Overshoot (%)	Steady state error(%)
RCAH-Baseline	2.86	4.93	0.01	0.607
ACAH-Baseline	2.83	5.16	0.01	0.677
TRC-Baseline	2.76	5.31	0.04	1.155

Time history of vehicle states and control inputs are shown from Figure 8 to Figure 10. Time history of vehicle states shows that vehicle states and control inputs of different control modes coincide very well, but it demonstrates that the outputs of the RCAH mode oscillate the most and generally reach the largest values as well. The TRC mode oscillates the least, followed by ACAH. This also applies to the value of the states. They all meet the requirements for flying tasks. Therefore, the pilot control strategy utilized in accomplishing this flying tasks is appropriate rather than aggressive.

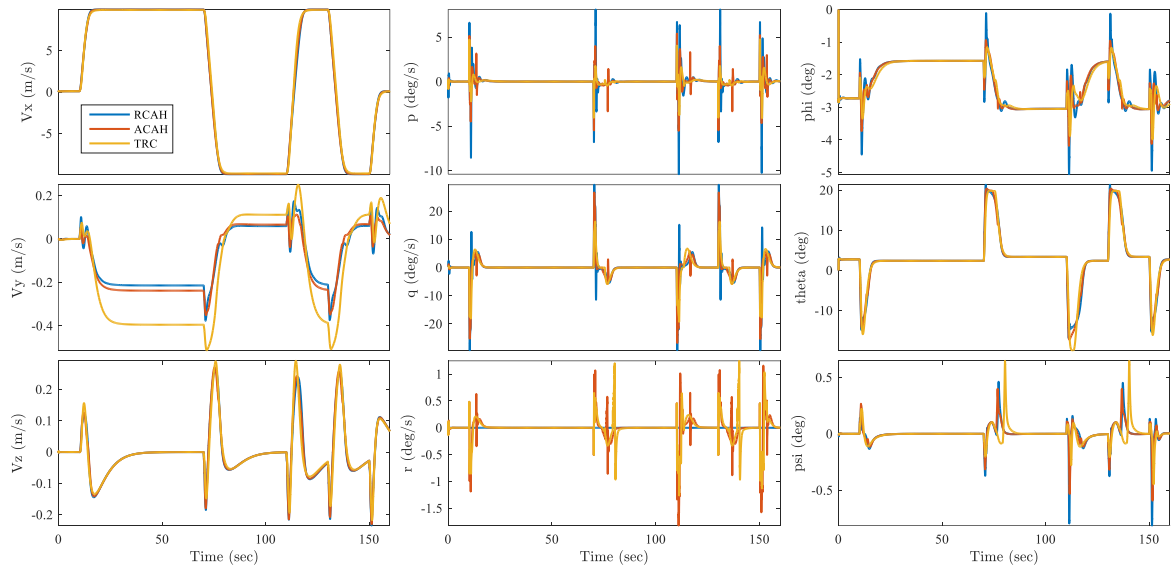

Figure 8. Time history of vehicle states

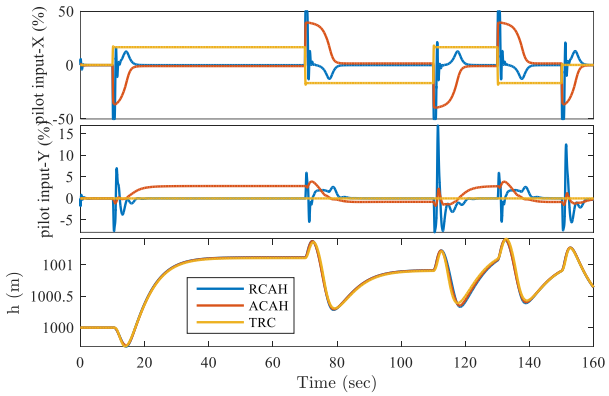

Figure 9. Time history of pilot inputs and altitude

Presented at 45th European Rotorcraft Forum, Warsaw, Poland, 17-20 September 2019

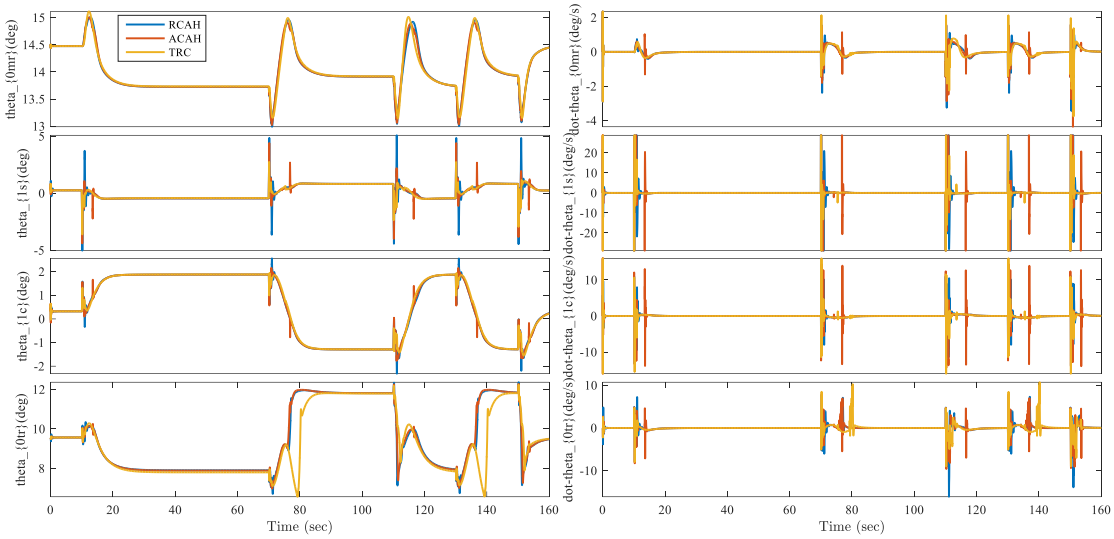

Figure 10. Time history of control inputs and derivatives

4.1.3 Multi-axis ROVER detection results

The threshold values for ROVER in this research are listed in Table 6. PIO detection results of RCAH, ACAH and TRC mode baselines are listed in Figure 11 to Figure 13 (Different colours represent different single-Rover detection results). From the results, one can see that they are all PIO free. The ROVER score corresponds to the variation of the forward ground velocity very well (actually, it is the variation of all the vehicle states, here the forward ground velocity is used as an example to show this variation.) As the round dot in the ROVER score figures represents the effective oscillation of the vehicle states and pilot inputs, one can conclude that the RCAH mode has the most oscillations, the ACAH mode follows and the TRC mode oscillates the least, which is in accordance with the time histories of the vehicle states (Figure 8 to Figure 10). From TRC to ACAH to RCAH mode, the number of ROVER flag equalling 3 and 3.5 is increasing, which indicates that the RCAH mode is more PIO prone than the other two control modes and that the TRC mode is the least PIO prone.

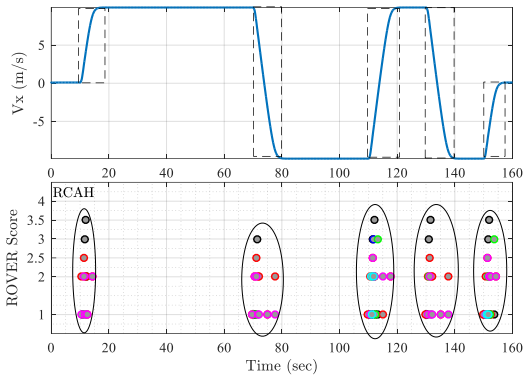

Figure 11. Multi-ROVER detection results of the RCAH Baseline

Table 6. Threshold values for ROVER

Threshold name	Value	Unit
Stick peak to peak amplitude (RCAH,ACAH)	10	%
Stick peak to peak amplitude (TRC)	1	%
Angular rates peak to peak amplitude	25	deg/s
Oscillation frequency	1 to 8	Rad/s
Phase lag	80 to 180	deg

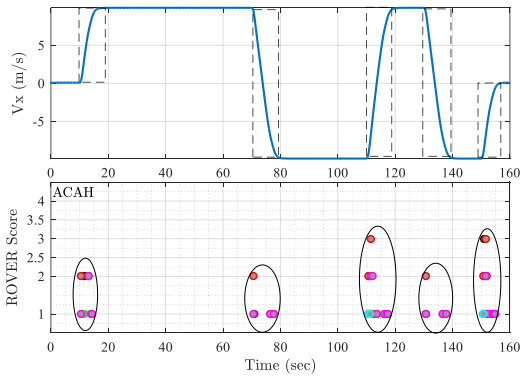

Figure 12. Multi- ROVER detection results of the ACAH Baseline

Presented at 45th European Rotorcraft Forum, Warsaw, Poland, 17-20 September 2019

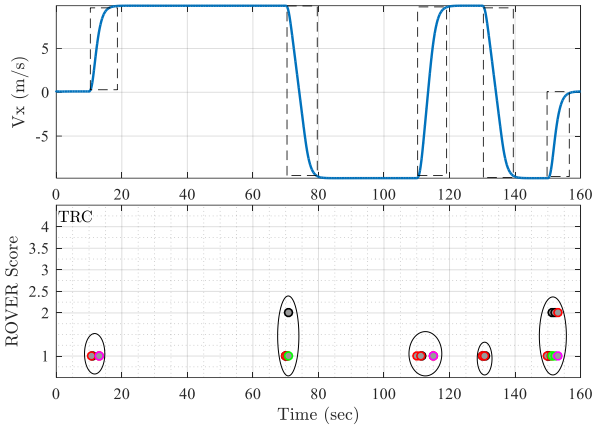

Figure 13. Multi- ROVER detection results of the TRC Baseline

4.2 Sensitivity to Pilot time delay

It is known that pilot time delay aggravates the occurrence of PIO. However, how pilot time delay acts on different control modes is unclear. Thus, some cases are investigated in this study to reveal the sensitivity of different control modes to pilot time delay. For this analysis all settings are the same as in the baseline cases of RCAH, ACAH and TRC modes, except the pilot time delay.

The multi-axis ROVER detection results of different control modes are summarized in Table 7. In order to have a good comparison, the results of the ROVER flag equalling 3, 3.5 and 4 are depicted in Figure 14.

For the RCAH mode, when the pilot time delay increases to 0.2 seconds, PIO occurs. With the increase of pilot time delay, oscillations (round dots) are increasing. For the ACAH mode, the general situation is similar, but only when the pilot time delay reaches 2.9 seconds does PIO occur. For the TRC mode, pilot time delay has no influence on PIO. To sum up, the TRC mode is not sensitive to pilot time delay with the baseline settings. The ACAH mode with baseline settings can tolerate large pilot time delays. Pilot time delay reaching up to 2.9 seconds can be regarded as pilot error, and in this case, it is the pilot to blame, rather than the vehicle systems, which makes the pilot time delay in these cases an external trigger event. The RCAH mode is most sensitive to pilot time delay. Even a small pilot time delay (0.1s) can trigger PIO. The reason why RCAH mode is the most sensitive to pilot time delay is that, in RCAH mode, angular rates follow pilot control input, so pilot time delay will affect angular rates, attitude angles and velocities, while for the ACAH mode, pilot time delay will only affect attitude angles and velocities and for the TRC mode pilot time delay only affect velocities. Thus the influence of pilot time delay on PIO's in the different control modes reduces from RCAH to ACAH and to TRC.

To verify the effectiveness of the multi-axis Rover detection method, the RCAH mode with 0.2 seconds pilot time delay is given as an example. Figure 15 to Figure 23 show the single-axis ROVER detection results, they are respectively: from longitudinal pilot input to roll rate, longitudinal pilot input to pitch rate, longitudinal pilot input to yaw rate, lateral pilot input to roll rate, lateral pilot input to pitch rate and lateral pilot input to yaw rate. In Figure 15, one can see that the longitudinal pilot input is out of phase with roll rate, the longitudinal pilot input is large enough to be noted, and the oscillation frequency is within the range of PIO frequency. As a result, the ROVER flags equals 3.5. It is a precursor of PIO, which indicates that PIO may occur, but currently it is still PIO free. When the roll rate is large enough then flag 4 (PIO) appears. Figure 17 and Figure 20 have a similar situation as in Figure 15 except that the yaw rate is very small. Figure 16, Figure 18 and Figure 19 lack the most important characteristics of PIO, since the pilot input and vehicle states are not out of phase. In this case, even though the pilot input and vehicle states are large enough, and the oscillation frequency is located in the PIO frequency range, there will be no PIO. Figure 21 and Figure 22 demonstrate the phase relationship between pilot input and vehicle states. The time history of the pilot inputs and angular rates confirms the results from the ROVER score. Figure 23 shows the Multi-axis ROVER results. It shows that Multi-axis ROVER can detect PIO accurately, corresponding to the obvious variation of vehicle states. In this case, it is the variation of roll angle and it is in accordance with results in Figure 15. Small oscillations correspond to continuous flags which equal 3.5, while large oscillations correspond to flags which equal 4.

To conclude, this case demonstrates the effectiveness of the multi-axis ROVER detection method. Not only can it detect the time when PIO occurs but it also can detect the variables that are having PIO and the pilot input that triggered the PIO. In addition, it shows that the helicopter couplings are severe.

Presented at 45th European Rotorcraft Forum, Warsaw, Poland, 17-20 September 2019

Table 7. Multi-axis ROVER detection results of sensitivity to pilot time delay

case	Pilot Time delay(s)	ROVER flags 1	2	2.5	3	3.5	4	PIO
RCAH	0	54	41	7	8	4	0	no
RCAH	0.1	78	68	34	15	11	0	no
RCAH	0.2(E)	52	326	384	157	124	4	yes
RCAH	0.3	188	466	249	82	59	46	yes
ACAH	0	49	14	0	3	0	0	no
ACAH	0.1	48	16	0	3	0	0	no
ACAH	0.2	49	13	0	3	0	0	no
ACAH	1	102	46	3	4	1	0	no
ACAH	2.8	154	472	3	15	1	0	no
ACAH	2.9	166	386	183	30	16	35	yes
TRC	0	25	4	0	0	0	0	no
TRC	0.1	25	4	0	0	0	0	no
TRC	5	25	4	0	0	0	0	no

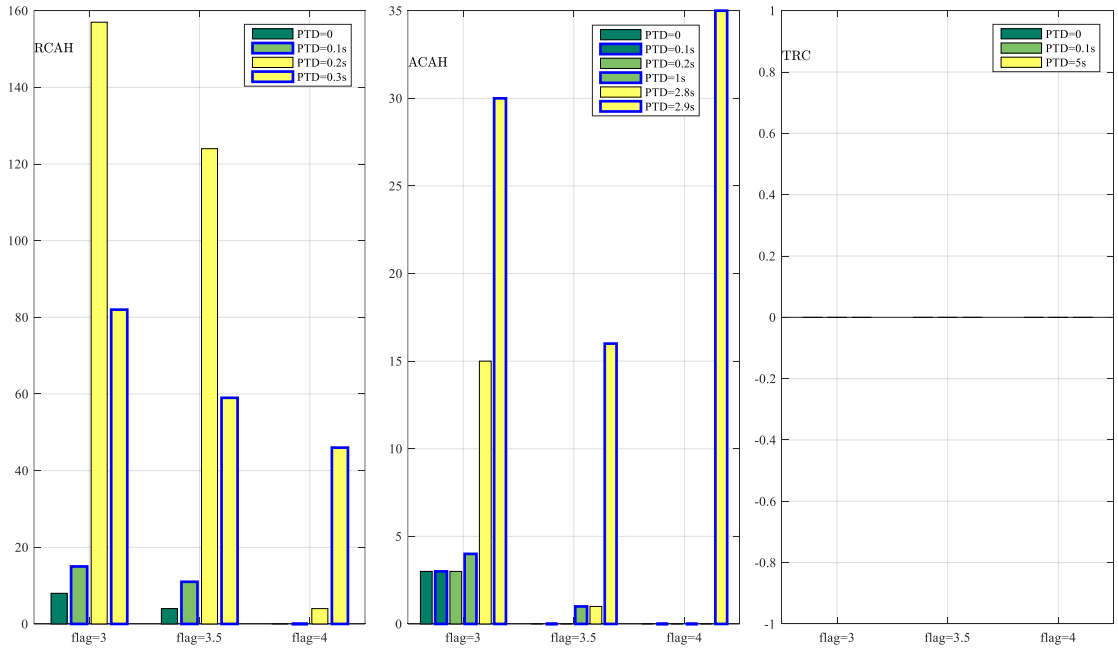

Figure 14. Multi-axis ROVER detection results of sensitivity to pilot time delay

Presented at 45th European Rotorcraft Forum, Warsaw, Poland, 17-20 September 2019

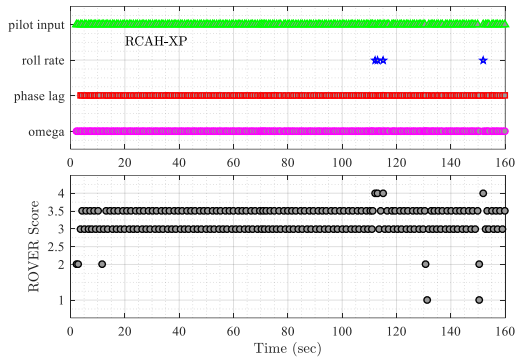

Figure 15. Single-axis ROVER detection results of RCAH mode when PTD=0.2s

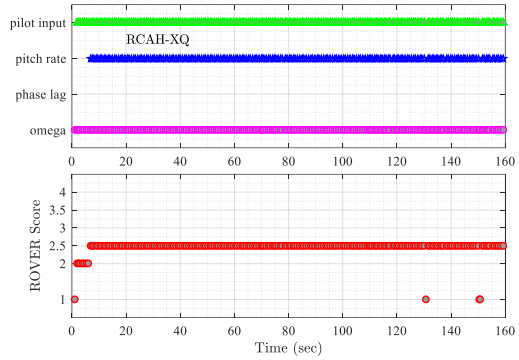

Figure 16. Single-axis ROVER detection results of RCAH mode when PTD=0.2s

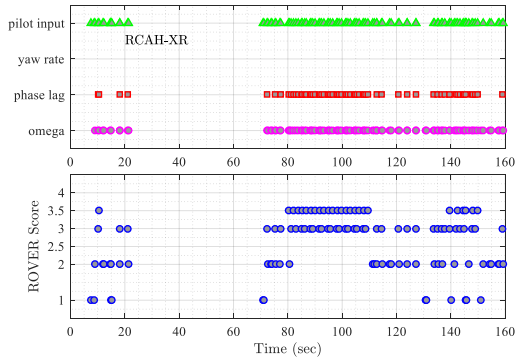

Figure 17. Single-axis ROVER detection results of RCAH mode when PTD=0.2s

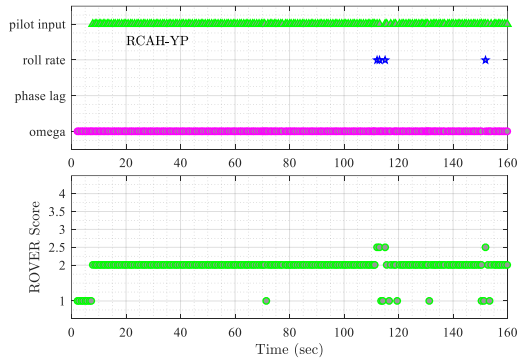

Figure 18. Single-axis ROVER detection results of RCAH mode when PTD=0.2s

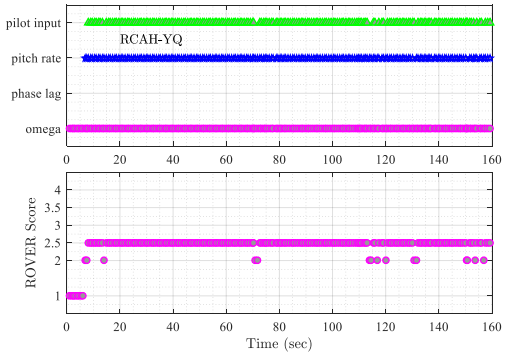

Figure 19. Single-axis ROVER detection results of RCAH mode when PTD=0.2s

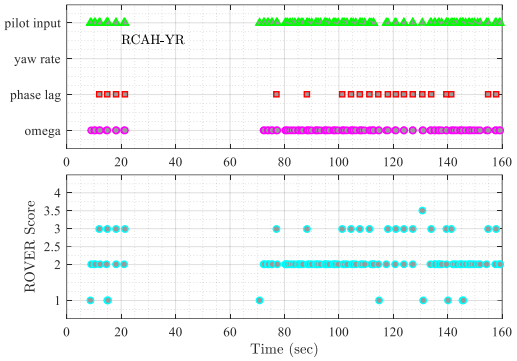

Figure 20. Single-axis ROVER detection results of RCAH mode when PTD=0.2s

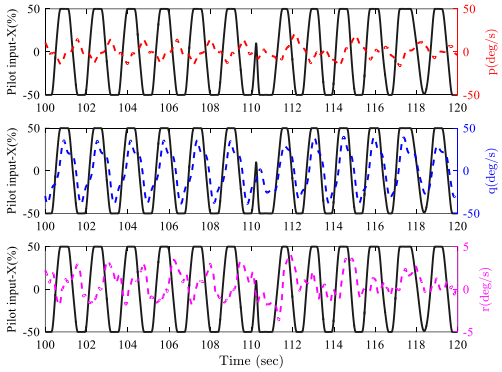

Figure 21. Time history of longitudinal pilot input and angular rates

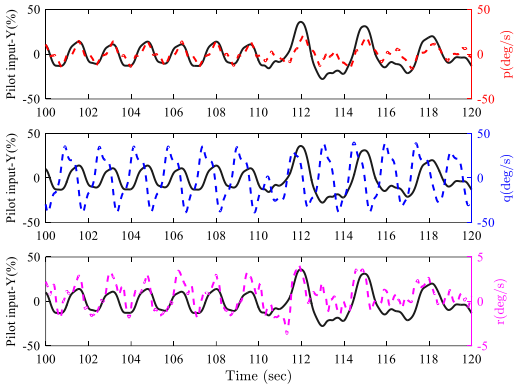

Figure 22. Time history of lateral pilot input and angular rates

Presented at 45th European Rotorcraft Forum, Warsaw, Poland, 17–19 September, 2019.

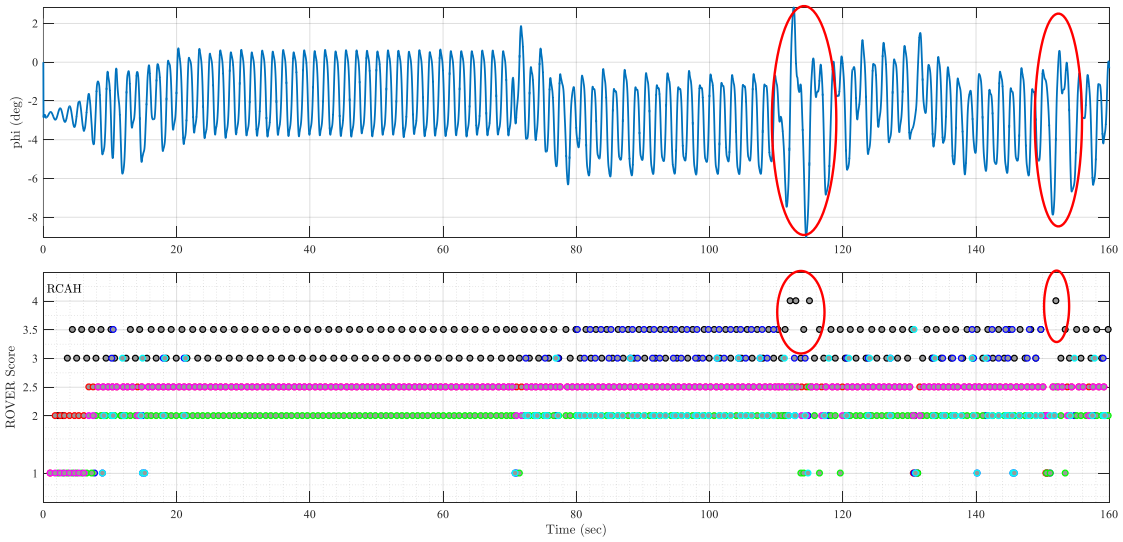

Figure 23. Multi-axis ROVER detection results of RCAH mode when PTD=0.2s

4.3 Sensitivity to actuator saturation

Actuator saturation is unavoidable in actual vehicles and the fact that actuator saturation can cause Cat. II PIO is well known. The tolerability of different control modes to actuator saturation is interesting. The following cases investigate control mode sensitivity to abnormal actuator saturation and the compound effect of pilot time delay. All the settings are the same as with the baseline cases of RCAH, ACAH and TRC, except for the actuator saturation value and the pilot time delay. The extra actuator saturation is only introduced to longitudinal and lateral control, while collective and tail rotor control are identical to the baseline. The Multi-axis ROVER results are shown in Table 8. Flags larger than 3 are depicted in Figure 24.

For the RCAH mode, without pilot time delay, when the actuator saturation drops to 33% of the actuator's physic limits (baseline value) there is no PIO, but when it continues dropping to 32% PIO appears. As a result, the tolerability of the RCAH mode is 33%. Since there is no pilot time delay in these two cases and the pilot control strategy is not aggressive, it is the inner vehicle trigger event of abnormal actuator saturation that leads to PIO. When the RCAH mode is on the edge of having PIO (33%), a small pilot time delay (0.1 seconds) aggravates it to PIO. However, when the abnormal actuator saturation decreases to 32%, adding pilot time delay keeps the PIO but the oscillations become less. It cannot be concluded that pilot time delay can alleviate the PIO severity caused by abnormal actuator saturation since ROVER does not give a standard to differentiate the severity of PIO. Furthermore, the compound effect of abnormal actuator saturation and the pilot time delay is very complex due to the high nonlinearities and coupled vehicle dynamics. Thirdly, the pilot time delay is an uncontrollable factor, thus increasing pilot time delay to alleviate PIO is meaningless.

Similar analysis shows that the tolerability of the ACAH mode is 33%. When the ACAH mode is on the edge of having PIO (33%), it is still not very sensitive to pilot time delay. There is no PIO until the pilot time delay is up to 1 second. This indicates that the inner vehicle trigger event of abnormal actuator saturation plays a leading role in triggering PIO. The compound effect of abnormal actuator saturation and the pilot time delay is similar to that of the RCAH mode. Compared with the case of 100% normal actuator saturation, the tolerability of ACAH to pilot time delay degrades. It decreases from 2.9 seconds to 1 second.

For the TRC mode, the tolerability to actuator saturation is 33%. When there is no PIO (with abnormal actuator saturation higher than 33%), TRC is not sensitive to pilot time delay. The compound effect of abnormal actuator saturation and pilot time delay is similar to that of the RCAH mode.

To sum up, the tolerability of different control modes to abnormal actuator saturation is the same (33%), which means that, when actuator saturation is the trigger event, PIO cannot be alleviated by changing control modes. The reason why the tolerance to abnormal actuator saturation is the same is that, as long as the flying tasks are the same, the required actuator position is the same regardless of control modes. When there is no PIO, the TRC mode has the highest tolerance to pilot time delay, followed by ACAH, while RCAH is the most sensitive one. With the abnormal actuator saturation, even if there is no PIO, the tolerability of ACAH and RCAH mode to pilot time delay degrades compared nominal actuator saturation.

Presented at 45th European Rotorcraft Forum, Warsaw, Poland, 17–19 September, 2019.

Table 8. Multi-axis ROVER detection results of sensitivity to actuator saturation and pilot time delay

case	Pilot Time delay(s)	Rate Limits (%)	ROVER flags						PIO
			1	2	2.5	3	3.5	4	
RCAH	0	33	75	59	8	13	5	0	no
RCAH	0.1	33	68	110	55	20	13	10	yes
RCAH	0	32	131	199	40	57	21	20	yes
RCAH	0.1	32	129	230	55	56	21	13	yes
ACAH	0	33	64	22	0	2	0	0	no
ACAH	0.1	33	64	24	0	2	0	0	no
ACAH	0.2	33	62	24	0	2	0	0	no
ACAH	0.9	33	116	134	14	20	1	0	no
ACAH	1	33	123	194	60	23	12	35	yes
ACAH	0	32	156	211	66	30	14	19	yes
ACAH	0.1	32	143	129	28	20	5	4	yes
TRC	0	33	25	7	0	0	0	0	no
TRC	0.1	33	25	7	0	0	0	0	no
TRC	5	33	25	7	0	0	0	0	no
TRC	0	32	261	192	9	21	7	2	yes
TRC	0.1	32	271	187	8	20	6	3	yes

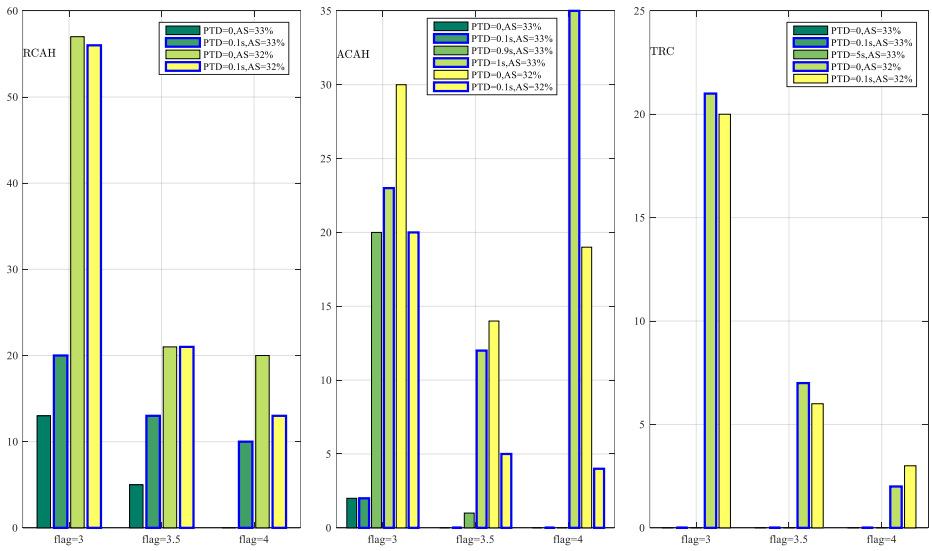

Figure 24. Multi-axis ROVER detection results of sensitivity to actuator saturation and pilot time delay

Presented at 45th European Rotorcraft Forum, Warsaw, Poland, 17–19 September, 2019.

4.4 Sensitivity to actuator rate limits

It is well known that the actuator rate limit is an important trigger event of Cat. II PIO. Therefore it is of great importance to study the tolerability of different control modes to actuator rate limits. The following cases study different control mode sensitivities to abnormal actuator rate limit and the compound effect of pilot time delay. Other than the actuator rate limit value and pilot time delay, the remaining settings are identical to the baseline cases of RCAH, ACAH, and TRC. The Multi-axis ROVER results are shown in Table 9.Similarly, flags larger than 3 are depicted in Figure 25.

For the RCAH mode, without pilot time delay, when the abnormal actuator rate limit descends to 76% of the actuator's physical limits (baseline value) there is no PIO, but when it continues to 75%, PIO occurs. As a consequence, the tolerability of RCAH mode to abnormal actuator rate limit is 76%. Since there is no pilot time delay in these two cases and the pilot control strategy is not aggressive, it is the inner vehicle trigger event abnormal actuator rate limit that leads to PIO. When the RCAH mode is on the edge of having PIO (76%), a small pilot time delay (0.1 seconds) aggravates it to PIO. With an existing PIO (actuator rate limit is 75% of the baseline value), a pilot time delay deteriorates the case as well.

The tolerability of ACAH to abnormal actuator rate limit is 35%. When the ACAH mode is on the edge of suffering from PIO (35%), its tolerance to pilot time delay decreases to less than 0.4 seconds. This implies that the abnormal actuator rate limit makes the ACAH mode more sensitive to pilot time delay, since in the baseline with 100% normal actuator rate limit, its resistance to pilot time delay is 2.9 seconds. It indicates that the inner vehicle trigger event abnormal actuator rate limit plays a leading role in triggering PIO as well.

The tolerability of TRC to abnormal actuator rate limit is 18%. When the abnormal actuator rate limit is not triggered (higher than 18%), the TRC mode is not sensitive to pilot time delay. However, when there is PIO, the pilot time delay will aggravate the developing of the PIO.

In summary, the tolerability of different control modes to abnormal actuator rate limit varies greatly. This indicates that it may be possible to alleviate PIO triggered by abnormal actuator rate limit by changing control modes. TRC mode has the highest tolerability to abnormal actuator rate limit, followed by ACAH and RCAH. It is because the activity of actuators of different control modes is different. According to the analysis of the baseline actuator activity, the RCAH mode actuators oscillates the most and reach the largest value, thus it is the most prone to reach the rate limit. That explains why the tolerance of the RCAH mode to abnormal actuator rate limit is the lowest. When there is no PIO, the TRC mode has the highest tolerance to pilot time delay, followed by ACAH and RCAH. With the abnormal actuator rate limit, even if it does not have a PIO, the tolerability of ACAH and RCAH mode to pilot time delay degrades compared to the baseline actuator rate limit.

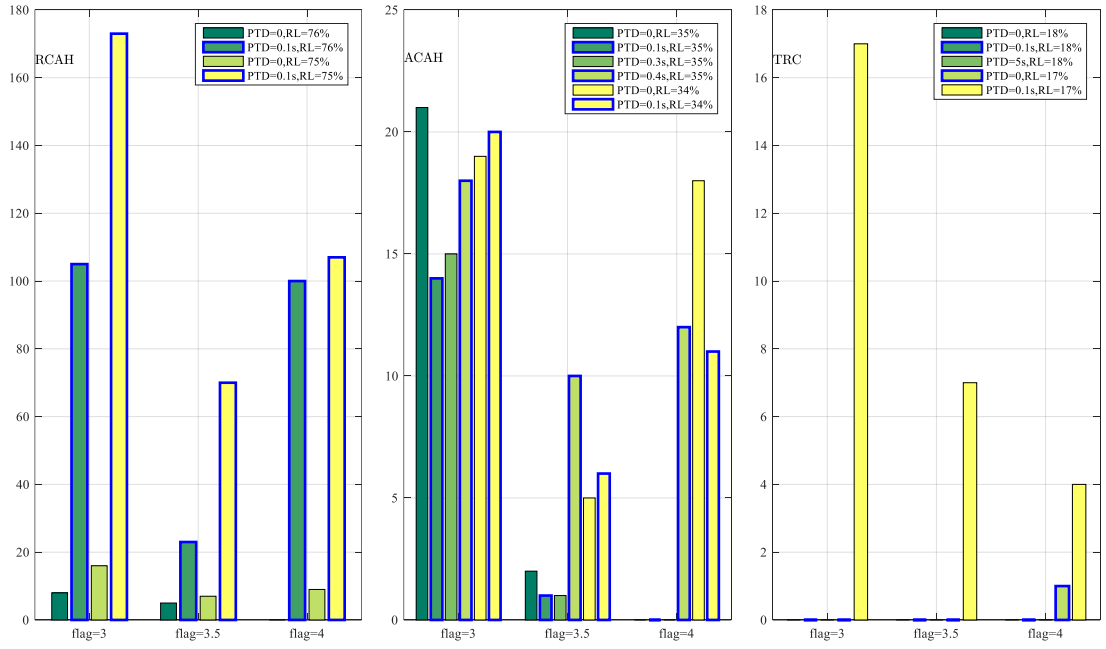

Figure 25. Multi-axis Rover detection results of sensitivity to actuator rate limit and pilot time delay

Presented at 45th European Rotorcraft Forum, Warsaw, Poland, 17–19 September, 2019.

Table 9. Multi-axis ROVER detection results of sensitivity to actuator rate limit and pilot time delay

case	Pilot Time delay(s)	Actuator Saturation (%)	ROVER flags						PIO
			1	2	2.5	3	3.5	4	
RCAH	0	76	49	64	11	8	5	0	no
RCAH	0.1	76	74	300	402	105	23	100	yes
RCAH	0	75	41	71	38	16	7	9	yes
RCAH	0.1	75	60	417	544	173	70	107	yes
ACAH	0	35	168	133	18	21	2	0	no
ACAH	0.1	35	147	83	11	14	1	0	no
ACAH	0.2	35	120	73	14	15	0	0	no
ACAH	0.3	35	150	103	17	15	1	0	no
ACAH	0.4	35	123	116	58	18	10	12	yes
ACAH	0	34	124	119	50	19	5	18	yes
ACAH	0.1	34	156	109	32	20	6	11	yes
TRC	0	18	55	27	5	0	0	0	no
TRC	0.1	18	57	31	6	0	0	0	no
TRC	5	18	48	20	4	0	0	0	no
TRC	0	17	59	47	21	0	0	1	yes
TRC	0.1	17	119	223	11	17	7	4	yes

4.5 Sensitivity to SCAS control authority

The control authority of the SCAS is a nonlinear element in the vehicle system, thus it has great potential to trigger PIO. In this section, the tolerability of different control modes to abnormal control authority of the SCAS as well as the compound effect of pilot time delay is investigated. Apart from the control authority value and pilot time delay, other settings are identical to the baseline cases of RCAH, ACAH and TRC. The reduced SCAS control authority is implemented by decreasing the saturation value of the nonlinear saturation element which represents the control authority. For example, when the control authority is 50%, this means that the saturation value is 50% of the nominal value. The Multi-axis ROVER results are shown in Table 10. Similarly, flags larger than 3 are depicted in Figure 26.

For the RCAH mode, without pilot time delay, when the abnormal control authority descends to 45% of the baseline value there is no PIO, but when it continues to 44%, PIO occurs. As a consequence, the tolerability of the RCAH mode to abnormal control authority is 45%. Since there is no pilot time delay in these two cases and the pilot control strategy is not aggressive, it is the inner vehicle trigger event abnormal control authority that leads to PIO. When the RCAH mode is on the edge of having PIO (45%), a small pilot time delay (0.1 seconds) aggravates it to PIO. However, when the abnormal control authority descends to 44% and PIO already exists, with pilot time delay, the PIO remains, but the oscillations become less.

The tolerability of ACAH to abnormal control authority is 37%. When the ACAH mode is on the edge of undergoing PIO (37%), its tolerance to pilot time delay reduces to less than 0.9 seconds. It implies that the abnormal control authority makes

Presented at 45th European Rotorcraft Forum, Warsaw, Poland, 17-20 September 2019

the ACAH mode more sensitive to pilot time delay, as, in the baseline with 100% normal control authority, its resistance to pilot time delay is 2.9 seconds. It indicates that the inner vehicle trigger event abnormal control authority plays a dominant role in triggering PIO as well.

The tolerability of TRC to abnormal control authority is 35%. When the abnormal control authority is not triggered (higher than 35%), the TRC mode is not sensitive to pilot time delay. However, when PIO exists, the pilot time delay will aggravate the development of PIO.

In conclusion, the tolerability of different control modes to abnormal control authority varies within 10% variations. This implies that changing control modes may be a way to alleviate PIO caused by abnormal control authority of the SCAS.TRC has the highest tolerability to the abnormal control authority, followed by ACAH and RCAH. The reason is a bit similar to that of the actuator rate limit. The control signals of the RCAH mode passing the SCAS oscillate the most and reach the largest value, which makes it the most prone to the saturation of control authority. Thus the tolerability of RCAH mode to abnormal control authority is the lowest. When there is no PIO, the TRC mode has the highest tolerance to pilot time delay, followed by ACAH and RCAH. With the abnormal control authority, though there is no PIO, the tolerability of ACAH and RCAH mode to pilot time delay degrades compared to the baseline of 100% normal control authority.

Table 10. Multi-axis ROVER detection results of sensitivity to control authority and pilot time delay

case	Pilot Time delay(s)	Control authority (%)	ROVER flags						PIO
			1	2	2.5	3	3.5	4	
RCAH	0	45	55	52	9	8	4	0	no
RCAH	0.1	45	135	98	25	19	11	1	yes
RCAH	0	44	103	149	19	34	18	7	yes
RCAH	0.1	44	117	118	26	31	22	2	yes
ACAH	0	37	65	26	2	5	1	0	no
ACAH	0.1	37	61	30	3	3	0	0	no
ACAH	0.2	37	61	28	2	2	0	0	no
ACAH	0.8	37	73	35	0	6	0	0	no
ACAH	0.9	37	122	156	66	34	19	30	yes
ACAH	0	36	78	53	6	4	2	1	yes
ACAH,	0.1	36	83	42	3	4	1	0	no
TRC	0	35	38	11	0	1	0	0	no
TRC	0.1	35	38	11	0	1	0	0	no
TRC	5	35	38	11	0	1	0	0	No
TRC	0	34	289	196	11	14	0	4	yes
TRC	0.1	34	285	199	11	14	0	4	yes

Presented at 45th European Rotorcraft Forum, Warsaw, Poland, 17-20 September 2019

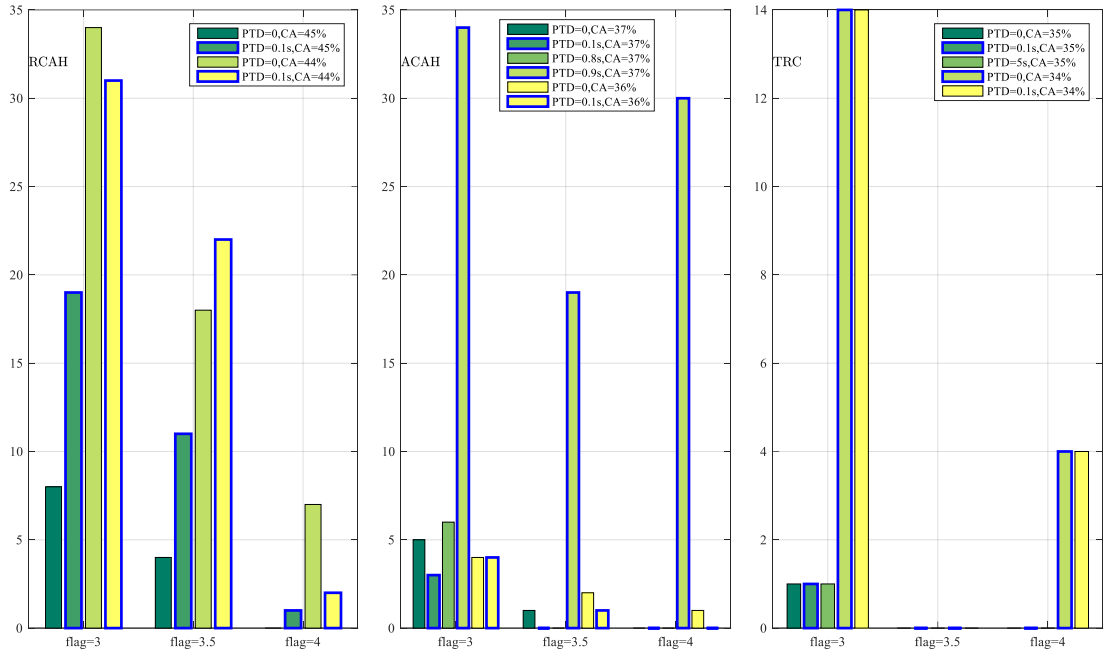

Figure 26. Multi-axis ROVER detection results of sensitivity to control authority and pilot time delay

4.6 Sensitivity to sensor dynamics

Sensor dynamics are important elements in the vehicle system, since all the feedback signals are obtained from them. If the difference between the actual values and the measured values is large enough, it may trigger PIO as it caused a mismatch in the vehicle system. In this section, the tolerability of different control modes to abnormal sensor dynamics as well as the compound effect of pilot time delay is studied. Except for the sensor dynamics value and pilot time delay, other settings are identical to the baseline cases of RCAH, ACAH and TRC modes. The Multi-axis ROVER results are shown in Table 11. Similarly, flags larger than 3 are depicted in Figure 27.

For the RCAH mode, without pilot time delay, when the abnormal sensor dynamics descend to 33% of the baseline value there is no PIO, but when it continues dropping to 32%, PIO occurs. As a result, the tolerability of RCAH to abnormal sensor dynamics is 33%. Since there is no pilot time delay in these two cases and pilot control strategy is not aggressive, it is the inner vehicle trigger event abnormal sensor dynamics that result in PIO. When the RCAH mode is on the edge of having PIO (33%), a small pilot time delay (0.1 seconds) aggravates it to PIO. However, when the abnormal sensor dynamics descends to 32% and PIO already exists and adding a pilot time delay, there remains to be PIO but the oscillations become less.

The tolerability of ACAH to abnormal sensor dynamics is 39%. When the ACAH mode is on the edge of undergoing PIO (39%), its tolerance to pilot time delay reduces to less than 0.8 seconds. It implies that the abnormal sensor dynamics makes the ACAH mode more sensitive to pilot time delay, as in the baseline with 100% normal sensor dynamics its resistance to pilot time delay is 2.9 seconds. It indicates that the inner vehicle trigger event abnormal sensor dynamics plays a dominant role in triggering PIO as well.

The tolerability of TRC to abnormal sensor dynamics is 33%. When the abnormal sensor dynamics is not triggered (higher than 33%), TRC is not sensitive to pilot time delay. However, when the abnormal sensor dynamics descends to 32% and PIO already exists and adding pilot time delay, there remains to be PIO but the oscillations become less.

In conclusion, the tolerability of different control modes to abnormal sensor dynamics varies, with only 7% variations. TRC and RCAH modes have the same tolerability to abnormal sensor dynamics while the ACAH mode has the lowest one. In this case, the tolerability does not show a positive correlation with the advanced level of control modes (From RCAH to ACAH to TRC, the level advances). It may be due to the complexity of the sensors. Thus, altering control modes may not be an effective measure to alleviate PIO triggered by abnormal sensor dynamics. When there is no PIO, the TRC mode has the highest tolerance to pilot time delay, and ACAH follows, while RCAH is the most sensitive one. With the abnormal sensor dynamics, though there is no PIO, the tolerability of ACAH and RCAH to pilot time delay degrades compared to the baseline of 100% normal sensor dynamics.

Presented at 45th European Rotorcraft Forum, Warsaw, Poland, 17-20 September 2019

Table 11. Multi-axis ROVER detection results of sensitivity to sensor dynamics and pilot time delay

Mode	Pilot Time delay(s)	Sensor dynamics ω_{sn} (rad/s)	ROVER flags						PIO
			1	2	2.5	3	3.5	4	
RCAH	0	33	64	53	9	9	5	0	no
RCAH	0.1	33	28	415	754	87	52	240	yes
RCAH	0	32	20	364	710	72	61	240	yes
RCAH	0.1	32	56	248	474	83	54	146	yes
ACAH	0	39	53	12	0	3	0	0	no
ACAH	0.1	39	48	16	0	3	0	0	no
ACAH	0.2	39	45	17	0	3	0	0	no
ACAH	0.7	39	61	17	4	3	2	0	no
ACAH	0.8	39	160	280	132	40	29	47	yes
ACAH	0	38	72	23	1	2	1	1	yes
ACAH	0.1	38	87	156	84	17	9	18	yes
TRC	0	33	26	9	0	1	0	0	no
TRC	0.1	33	26	9	0	1	0	0	no
TRC	5	33	26	9	0	1	0	0	no
TRC	0	32	321	201	8	13	5	6	yes
TRC	0.1	32	314	231	7	18	7	5	yes

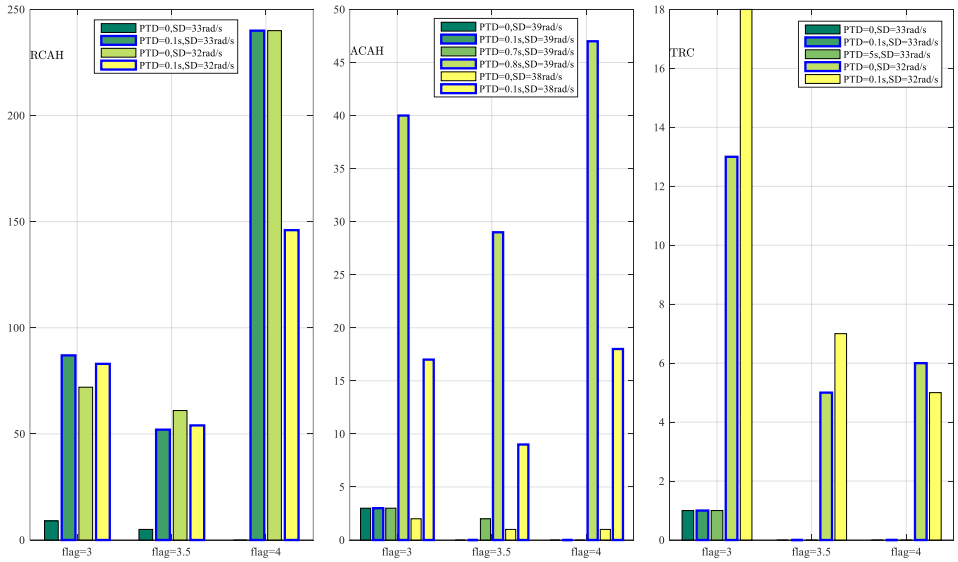

Figure 27. Multi-axis ROVER detection results of sensitivity to sensor dynamics and pilot time delay

Presented at 45th European Rotorcraft Forum, Warsaw, Poland, 17–19 September, 2019.

4.7 Validation example-sensor dynamics

As described in ADS-33E-PRF, degradation of the Bandwidth criteria may be an indication of a PIO prone configuration of the vehicle. Since the vehicle system in this research is nonlinear and coupled, and other nonlinear elements (such as actuator rate limit, actuator saturation, control authority) cannot be directly represented by a transfer function, it is difficult to obtain a frequency response. Thus, in this research, only the sensor dynamics are taken as an example to analyse the variation of bandwidth parameters. The linearization is implemented at the initial moment of the simulation. Here, we choose the abnormal sensor dynamics of RCAH and ACAH that triggered PIO to compare with the baseline. The bandwidth criteria parameters are calculated and listed in Table 12.

From the results, one can see that, compared to the baseline, the bandwidth of the PIO cases decrease and the phase delay increases. This indicates that the handling qualities of the cases with PIO do degrade, which corresponds to the description in ADS-33 well.

Table 12. Bandwidth criteria results of baseline and PIO cases

case	ω_{BWgain} (rad/s)	$\omega_{BWphase}$ (rad/s)	ω_{BW} (rad/s)	Phase delay τ_{bp} (s)
RCAH-SD100 (longitudinal)	7.57	8.56	7.57	0.04
RCAH-SD100 (lateral)	4.40	23.69	4.40	0.04
RCAH-SD32 (longitudinal)	3.45	8.15	3.45	0.09
RCAH-SD32 (lateral)	1.85	20.81	1.85	0.06
ACAH-SD100 (longitudinal)	7.80	8.73	8.73	0.04
ACAH-SD100 (lateral)	5.54	21.63	21.63	0.04
ACAH-SD38 (longitudinal)	4.13	8.36	8.36	0.08
ACAH-SD38 (lateral)	2.8559	19.7210	19.7210	0.06

5. Conclusions

Concluding, this research studies different control mode (RCAH, ACAH and TRC mode) sensitivity and tolerability to several PIO trigger factors (pilot time delay, actuator saturation, actuator rate limit, control authority of SCAS and sensor dynamics). The results on the above control modes analysis demonstrate that:

- When there is no PIO, the TRC mode has the highest tolerance to pilot time delay (TRC is not sensitive to pilot time delay), followed by ACAH, while RCAH is the most sensitive one.
- The pilot time delay is an external trigger factor, while actuator saturation, actuator rate limit, control authority of SCAS and sensor dynamics are inner vehicle trigger factors. Inner vehicle trigger factors play a leading role in triggering PIO.
- With any inner vehicle trigger factor, even when there is no PIO, the tolerability of ACAH and RCAH to pilot time delay degrades compared to the baseline. This implies that inner vehicle trigger factors make the RCAH, ACAH and TRC modes more sensitive to pilot time delay. However, the tolerance to pilot time delay from high to low remains to be TRC to ACAH to RCAH.
- The tolerability of different control modes to abnormal actuator saturation is the same (33%), which means that, when actuator saturation is the trigger event, PIO cannot be alleviated by changing control modes.
- The tolerability of different control modes to abnormal actuator rate limit varies greatly (RCAH 76%, ACAH 35%, TRC 18%, the higher the value, the lower the tolerance). This indicates that it may be possible to alleviate PIO triggered by abnormal actuator rate limit by changing control modes. However, one should be careful with this tactic since mode switching is known to be a potential trigger for PIO especially when this transition occurred unintentionally[20]. The mode switching used in this paper refers to the one that is manipulated by the pilot actively. Whether this could be an effective measure to alleviate PIO needs further study.
- The tolerability of different control modes to abnormal control authority varies (RCAH 45%, ACAH 37%, TRC 35%). This implies that changing control modes may be a way to alleviate PIO caused by abnormal control

Presented at 45th European Rotorcraft Forum, Warsaw, Poland, 17–19 September, 2019.

authority of the SCAS. Similar to abnormal rate limit trigger events, its effectiveness needs further evaluation by simulator experiments with the pilot in the loop.

- The tolerability of different control modes to abnormal sensor dynamics varies (RCAH 33rad/s, ACAH 39rad/s, TRC 33rad/s). TRC and RCAH have the same tolerability to abnormal sensor dynamics while ACAH has the lower one. In this case, the tolerability does not show a positive correlation with the advanced level of control modes (from RCAH to ACAH to TRC, the level advances). Thus, altering control modes may not be an effective measure to alleviate PIO triggered by abnormal sensor dynamics.

Although the results obtained from this research are based on the MATLAB simulation environment, conclusions can still have some guiding function for piloted simulator experiments. The next step is to implement experiments in the SIMONA simulator at TUDelft with human pilots to verify these results. With the HQR and PIOR given by human pilots involving experiments, more accurate PIO detection results can be obtained. Furthermore, the detection methods based on ROVER should be improved to give more accurate results in accordance with human pilots' detection results. The function of differentiating slight, moderate, severe or divergent PIO is needed as well. Last but not least, the role that mode transition plays in triggering PIO is another interesting issue to be investigated.

Acknowledgements

This study has been carried out in the context of the European Joint Doctorate NITROS (Network for Innovative Training on Rotorcraft Safety) project, whose main goal is to enhance rotorcraft safety by addressing critical aspects of their design. This project has received fundings from the European Union's Horizon 2020 research and innovation programme under the Marie Skłodowska-Curie grant agreement No. 721920.

References

[1] U.S.JHSAT (2011). The Compendium Report: The U.S. JHSAT Baseline of Helicopter Accident Analysis (1, pp.).

[2] U.S.JHSAT (2011). The Compendium Report: The U.S. JHSAT Baseline of Helicopter Accident Analysis (2, pp.).

[3] Yilmaz, D. (2018). Identifiation of Manual Control Behaviour to Assess Rotorcraft Handling Qualities, Delft University of Technology.

[4] Mcruer, D. T. (1997). AVIATION SAFETY AND PILOT CONTROL: UNDERSTANDING AND PREVENTING UNFAVORABLE PILOT-VEHICLE INTERACTIONS. Washington D.c.national Research Council National Academy

[5] Mcruer, D., Klyde, D., & Myers, T. (2013). Development of a comprehensive PIO theory. Paper presented at the Aiaa Atmospheric Flight Mechanics Conference.

[6] Fasiello, S., Yu, Y., Jump, M., Pavel, M. D., van Kampen, E.,... Masarati, P. (2018). Rotorcraft-Pilot Couplings: Analysis and Detection in a Safety Enhancement Framework. Paper presented at the Proceedings of the 44th European rotorcraft forum, Delft, The Netherlands.

[7] Pavel, M. D., Jump, M., Masarati, P., Zaichik, L., Dang-Vu, B., Smaili, H.,... Johnes, M. (2015). Practises to identify and prevent adverse aircraft-and-rotorcraft-pilot couplings—A ground simulator perspective. Progress in Aerospace Sciences, 77, 54-87.

[8] Jones, M. G. (2015). Prediction, Detection and Observation of Rotorcraft Pilot Couplings., University of Liverpool.

[9] van der Groot, R. R. (2017). Helicopter Control Using Incremental Adaptive Backstepping., Delft University of Technology.

[10] Baskett, B. J. (2000). Aeronautical Design Standard Performance Specification Handling Qualities Requirements For Military Rotorcraft .

[11] Liu, Q. (2012). Pilot-induced oscillation detection and mitigation. Cranfield University .

[12] Perfect, P., Jump, M., & White., M. D. (2012). Development of Handling Qualities Requirements for a Personal Aerial Vehicle. Paper presented at the Proceedings of the 38th European rotorcraft forum, Amsterdam, The Netherlands .

[13] Mitchell, D. G., & Hoh, R. H. (2000). Development of Methods and Devices to Predict and Prevent Pilot-Induced Oscillations. AFRL-VA-WP-TR-2000-3046.

[14] Mitchell, D., & Klyde, D. (2013). Recommended Practices for Exposing Pilot-Induced Oscillations or Tendencies in the Development Process. Aiaa Journal.

[15] Suliman, S. M. T., Yilmaz, D., & Pavel, M. D. (2012). Harmonizing Real-Time Oscilation Verifier (ROVER) with Handling Qualities Assesment for Enhanced Rotorcraft Pilot Couplings Detection. Paper presented at the Proceedings of the 38th

Presented at 45th European Rotorcraft Forum, Warsaw, Poland, 17-20 September 2019

European rotorcraft forum, Amsterdam,The Netherlands.

[16] Jirgl, M., Havlikova, M., & Bradac, Z. (2015). The Dynamic Pilot Behavioral Models. Procedia Engineering, 100, 1192-1197.

[17] Mitchell, D. G., & Hoh, R. H. (2000). Development of Methods and Devices to Predict and Prevent Pilot-Induced Oscillations. AFRL-VA-WP-TR-2000-3046 .

[18] Chalk, C. R. C. (1995). Presentation of PIO and the Effects of Rate Limiting. Flight Vehicle Integration Panel Workshop on Pilot Induced Oscillations (11-12): Advisory Group for Aerospace Research and Development

[19] Gray, W., \Boundary-avoidance tracking: A new pilot tracking model," AIAA Atmospheric Flight Mechanics Conference, United States Air Force Test Pilot School, Edwards AFB, CA 93524, San Francisco, CA, 15-18 August 2005, pp. 86-97.

[20] J. Moorhouse, D. (2001). Flight Control Design Best Practices Relative to Active Control Technology

Presented at 45th European Rotorcraft Forum, Warsaw, Poland, 17-20 September 2019